J. Mod. Transport. (2015) 23(2):137–147
DOI 10.1007/s40534-015-0070-6

www.springer.com/40534

Measurement methods and analysis tools for rail irregularities: a case study for urban tram track

Laura Chiacchiari · Giuseppe Loprencipe

Received: 17 October 2014 / Revised: 14 March 2015 / Accepted: 17 March 2015 / Published online: 18 April 2015

Abstract Rail irregularities, in particular for urban railway infrastructures, are one of the main causes for the generation of noise and vibrations. In addition, repetitive loading may also lead to decay of the structural elements of the rolling stock. This further causes an increase in maintenance costs and reduction of service life. Monitoring these defects on a periodic basis enables the network rail managers to apply proactive measures to limit further damage. This paper discusses the measurement methods for rail corrugation with particular regard to the analysis tools for evaluating the thresholds of acceptability in relation to the tramway Italian transport system. Furthermore, a method of analysis has been proposed: an application of the methodology used for treating road profiles has been also utilized for the data processing of rail profilometric data.

Keywords Rail corrugation · Noise disturbance · Measurement methods · Continuous measurement · Data processing algorithm · Wavebands filtering

1 Introduction

The interaction between rail and wheel influences safety and efficiency of railway service. The knowledge in contact phenomena, in both the surface characteristics and the contact mechanics [1, 2], may improve the accuracy in evaluating wheel–rail contact functional performance, and ensure the related prediction of local stresses. High vertical contact forces, also with the lateral and longitudinal ones, induce stresses that may produce fatigue failure of the material [3]. High contact stresses and rolling resistance induce friction heating and consequently wear [4]. Thus, traction and braking may lead to wheel sliding, which results in rail burn, wheel flat, unfavorable material phase transformation, and thermal cracks [5]. In addition to wear, fatigue, crack formation, and other permanent deformations, there is a particular type of defect which affects the rail surface called "Rail Corrugation". This is a kind of periodic wear that is often visible with the naked eyes and can be identified as the pattern on the rail has regular spacing.

In the contact area between rail and wheel, dynamic forces are exchanged: it has been noted that if the dynamic contact forces are high, then the level of corrugation will be high (though with a phase lag of around 135°) [4–9].

These dynamic phenomena may generate corrugation of the rails and the wheels and they can also cause the formation of different types of irregularities. This results in poor vehicle dynamics (when passing on a worn rail) and consequently higher contact forces, vibrations, and noises. Also in the case of perfectly smooth rail surface, this phenomenon appears as a consequence of the track discontinuities for the sleepers present (regularly spaced).

2 Literature review

Due to the contact between the wheels and rail surfaces, the train's motion on a track creates complex dynamic phenomena in the train itself and in the track's superstructure, which generates noise and vibrations that propagate in the external environment. These phenomena cause a service life reduction in all the structural components involved, an

L. Chiacchiari · G. Loprencipe (✉)
Dipartimento di Ingegneria Civile e Ambientale, Sapienza, Università di Roma, via Eudossiana, 18, 00184 Rome, Italy
e-mail: giuseppe.loprencipe@uniroma1.it

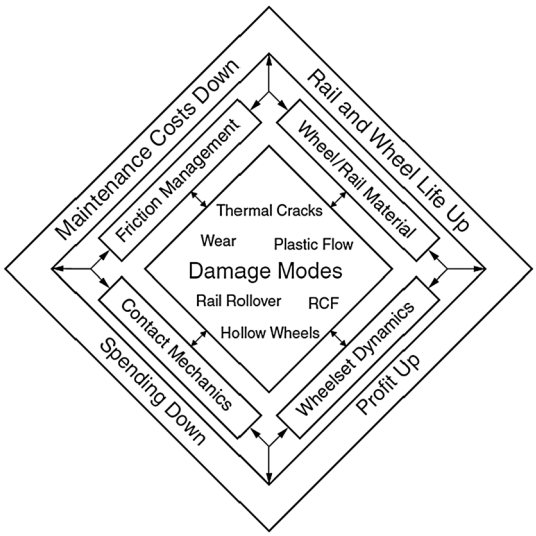

Fig. 1 Systems approach to wheel–rail interface research and development [10]

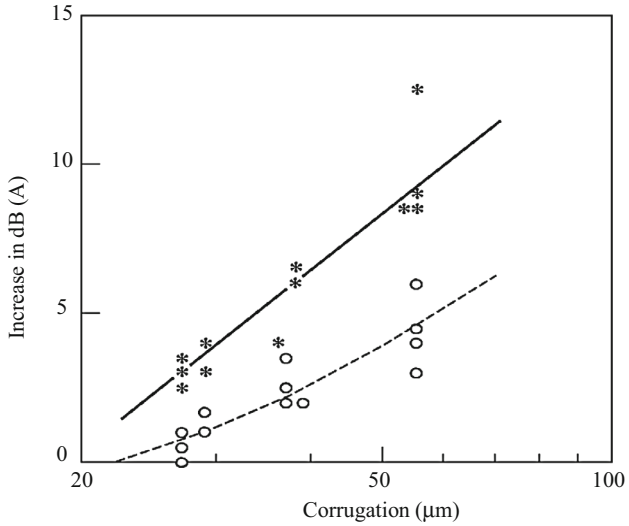

Fig. 2 Correlation between corrugation height and noise [11]

external disturbance in the receptors, and the decay of the passengers comfort. Figure 1 shows a scheme for the systematic approach to wheel–rail interface research and development: the figure illustrates that it is essential to take into account the combination of all the following aspects: contact mechanics, materials, dynamics, as well as friction. A proper study of this scheme can guarantee profitable optimizations for the management of the wheel–rail system interface.

Imperfections that occur at the wheel/rail contact, due to geometrical changes in the shape of rail and wheel surfaces, influence the stress distribution. In fact, the presence of these imperfections alters the pressure in the contact nominal area; this generated dynamic stress excites all the elements of the rail track system and propagates from the track through the ground, in the range of frequency excitation. Railhead irregularities occur on the surface of the rail: the profile can be worn, the railhead damaged by cracks from rolling contact fatigue phenomenon (RCF) [6], squats can take place [7], and further, short-pitch corrugation and rail welds create periodic occurrences [8, 9]. The rail corrugation on rail surface is very frequent in all railway infrastructures and is also classified as *short-wave defect* (*long wavelength irregularities* are, instead, defined as irregularities of wavelengths of 300 mm or longer, that may be either geometric irregularities in the track or on the wheel, or irregularities of the track stiffness [10]).

The importance of amplitude and wavelength dimension of rail corrugation has been demonstrated in many references. A clear correlation between the size of the railhead running surface irregularities and levels of generated noise and vibration was found by Thompson, [11] (see Fig. 2). In addition, because the correlation is related to dynamics aspects, the occurrence of defects is related to the train speed [4–8].

Rail corrugation, also known by the term short-pitch corrugation, frequently appears in straight track, where traction or braking is particularly severe, or in small radius curves, although it may also be detected in curves of greater radius. Therefore, in urban rail transport system this problem appears frequently, especially for tram networks, which present the following critical situations:

1. very accentuated wear due to exposition at both railway vehicles and other categories of traffic;
2. specific geometry of the tram line that offers particular conditions for the establishment of disturbance phenomena and wear;
3. location of tracks near noise-sensitive regions.

In addition, the insertion of rolling stock in this scenario contributes to developing wear: maintenance cycles lead to an uncontrolled increase in management costs that nullifies all the advantages of this transport system.

The geometry of this kind of irregularity, similar to waveform, is periodical and changes with different situations. A useful classification of the corrugations (irregularity wavelengths less than 1 m) is performed by grouping wavelength (λ) ranges:

- 10–30 mm;
- 30–100 mm;
- 100–300 mm;
- 300–1000 mm.

Rail corrugation appears to have a small wavelength when compared with the longitudinal waves of the rail.

During vehicle/track interaction, the forces are transmitted in the wheel/rail contact area: dynamic behavior is

found in a wide band, ranging from very low frequencies of 0.5–1 Hz for lateral and vertical car body accelerations, to 2000 Hz, as a consequence of geometrical irregularities in rail and wheel contact. This latter portion of high-frequency excitation content typically falls in the audible frequency range, inducing the most relevant contribution to rolling noise.

Along with other contact issues, rail corrugation is a severe problem for many tramway administrations, therefore short wavelength corrugation is the major focus of this paper.

Due to the tram speed, and according to the relation between the frequencies f and the train speed V, $f = V/\lambda$, the wavelength λ on a tram rail surface is commonly around 10–50 mm.

Since the vehicle/track interaction produces a wide-ranging vibratory phenomenon, this results in different types of noise: besides the rolling noise, the ground-borne noise and the structure-borne noise are generated as reflection of ground-borne vibration [12]. In general, the effect of ground-borne vibration is related to people discomfort (high-frequency vibration affects concentration ability, low-frequency vibration may cause muscular or internal organ injury, both depending on exposure time), rather than damage to buildings. Noise limitation can avoid structural damage of the buildings, but is also important to prevent fatigue damage due to cyclical vibration [13–16].

3 Rail corrugation: types and causes of formation

The phenomenon of rail corrugation occurs in all rail systems, with different sizes and naturally takes place even when smooth contact surfaces are involved. In this way, Grassie [17] proposed two distinct mechanisms for the generation of dynamic actions (Fig. 3). The first is called wavelength-fixing mechanism, that appears also in the case of ideal geometrical contact as a consequence of structural discontinuities in railway track configuration (e.g., as rails are mounted on discrete supports, the sleepers). For this reason, dynamic loads arise altering the wheel–rail interaction, regardless of the geometric imperfections on the rolling railhead surface. These dynamic forces propagate in

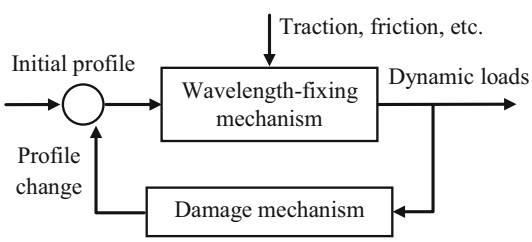

Fig. 3 A general corrugation mechanism [19]

all the train and track structural components, determining damage mechanism that occurs primarily on the wheel–rail contact surfaces. In consequence, permanent deformations on rolling surface are generated and gradually increases the generation of the dynamic forces in next train passages.

Irregularities present on wheel surface, will not be involved in this study (for which refer i.e., [18]). Both the generation and distribution of rail surface irregularities have a random nature.

Like irregularities of the road pavements, using appropriate instruments riding on the surface of the rail, measurements of profiles can be collected. These measurements show the variability of the irregularities of a longitudinal section of the rail surface compared to an ideal plane of reference. A proper analysis of the profiles allows to define the reference levels of rail degradation, and ensures to relate them to damage mechanisms, corrective solutions, levels of generation of noise and vibration, etc.

These longitudinal irregularities can be attributed to the following causes:

- pinned–pinned resonance,
- rutting due to second torsional resonance,
- P2 resonances.

The first type of wear is caused by pinned–pinned resonance of a track vibration, occurs mostly in straight tracks (indifferently on two rails), and in high rail of curves, especially in curves of greater radius, as consequence of the vibration of the rail bounded into two sleepers. This kind of corrugation may also appear in the track for light axle load traffic (less than 200 kN). Furthermore, in some circumstances, this defect is more evident in the correspondence of the sleepers [19].

The second type of corrugation occurs primarily in curves (on the inner rails) and in straight tracks often subject to traction or braking particularly severe. The name "rutting" was chosen because of the characteristic transverse grooves ("ruts") on the railhead [20]. The presence of local imperfections, as welds and joints, acts like triggering factor, determining the position of the corrugation along the rail. The damage of the inner rail in the curve is caused by a mechanism of the driven axles [19]: the phenomenon starts when the one wheel traction ratio is close to the friction limit, thus causing the slip and then the oscillation of the other wheel in correspondence with the second natural frequency of torsional resonance [21], as shown in Fig. 4.

The result of this phenomenon is wear of the rail with a geometric wavy development, with uniform wavelengths and appearance, and depth that can quickly reach tenths of a millimeter [19].

The last generation cause of corrugation comes from P2 resonance and interests straight tracks and outer rails in

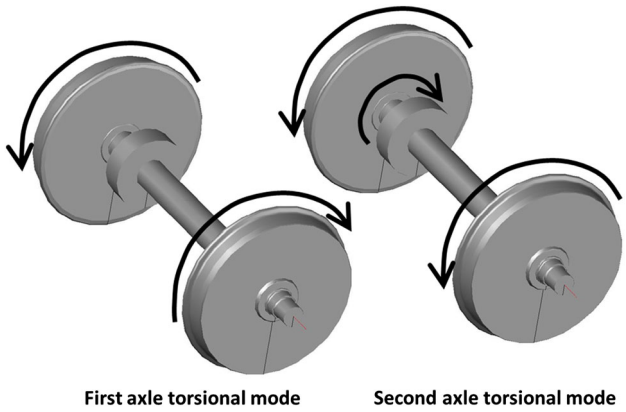

Fig. 4 Torsional resonances of wheelsets [19]

Fig. 5 Wear on tramway and railway tracks

curves: this kind of wear is mainly due to the vehicle "bouncing" on track, and the continuous vertical displacements of the wheelset, excited by the different stiffness that the unsprung masses perceive passing over discontinuities [22]. It occurs often on the tramlines (Fig. 5).

4 Measurement of rail irregularities

Corrugation is not a single phenomenon with a single cause and a single solution or treatment [20]. Cross studies should be effectuated to its right classification. The method to identify the causes is based on the survey of the damaged rail profile with appropriate instruments (Fig. 6).

In order to examine the longitudinal profiles of the rails, two different types of instrumentations are used:

- contact instruments;
- non-contact instruments.

The first are able to measure, one rail at a time, different part of a track, permitting to choose the length of each single measuring track and to select time by time the position of the sensor in the width of the railhead, guaranteeing extreme accuracy of 0.001 mm RMS (root mean square).

Fig. 6 Instruments for measuring the longitudinal profile of the rail (rail measurement)

The other ones, because mounted on vehicles of high speeds (5–140 km/h), record profiles of both rails simultaneously and provide uninterrupted measurements but with lower accuracy than the previous (0.003 mm RMS).

In addition, these instruments measure the irregularities under load and, therefore, in the same operating conditions of trains; however, they should solve the problem of inertial reference frame being vehicle-integrated measuring systems. This may cause some problem in finding the reference plane to which measurements of rail irregularities are referred.

For these reasons, contact instruments are generally preferred over the non-contact ones, to measure the longitudinal profiles of the rails.

The University of Cambridge and the British Rail Research [17] collaboratively developed the first model of CAT (Corrugation Analysis Trolley) in 1970 and then it was used in many railway infrastructures. This instrument, falling within the category of contact instrument, has a contact sensor (tip or roller sensor) and an odometer. The CAT works hand-pushed, riding the rail, allowing to detect the longitudinal profile on the surface of the rail with vertical precision of 0.01 μm [17]. This instrument, in addition to measuring the surface of the rail in terms of longitudinal profile, is able to return the acoustic roughness, the roughness of the rail connected to the generation of the noise (expressed in dB), and being provided with a dedicated software used for the calculation [23–25].

Another type of apparatus able to read rail profile, belonging to the category "not in contact", is the ORPMS (Optical Rail Profile Measurement System) that is based on optical triangulation realized through laser rays and assisted by mini cameras.

For the diagnosis of track defects during the last few years, several trains instrumented capable of continuous measurement and all the geometric parameters of interest including the profile of the rail, have been designed. For example the HSRCA system (High Speed Rail Corrugation Analyser), a not-in-contact system with Axle-box Accelerometers, is extremely reliable even at relatively high speeds (maximum recommended running speed of 120 km/h) [26].

Three different ways can be used to evaluate the condition of a rail surface starting from recorded profilometric

data: a method based on the spectral analysis, a method based on the assessments of percentage of exceeding, and expeditious methods.

5 Analysis of profilometric data by means of spectral analysis

The direct measurement and spectral analysis-based processing method form the basis of the shown resolution (Fig. 7). The presented algorithm is entirely in line with the UNI EN 15610:2009 one [27].

Method A determines the one-third octave band acoustic roughness spectrum $\tilde{r}(\lambda)$. The data must be processed to remove some unwanted "pit and spike", to adapt the measurement (if chosen) through an appropriate curvature processing that takes into account the particular roundness of the sensor adopted in the test measures, and at last, to apply the discrete Fourier transform (DFT) to the function determining power spectral density (PSD) in the frequency domain and produce a one-third octave level roughness spectrum as a function of wavelength averaging the magnitude suitably.

A detailed scheme for method A is shown in Fig. 7.

Localized rail defects are not significant in the assessment of the acoustic roughness related to the rolling noise component, therefore they should not be included in the application.

After removing moisture and other contamination from the railhead surface, determining the length along the rail of interest, the transverse width (w_{ref}), the relative distance to the field face of the rail (d_{ref}), and setting the instrument, the measurement can start.

According to Fig. 7, these are three steps to follow:

1. check data information to edit out the data relating to any rail joints, rail head defects, and welds, for not affecting the final spectrum analysis;
2. remove pits and spikes in the records;
3. correct the measure by the curvature processing that takes into account the form of the probe, before conducting spectral analysis.

The next step is to calculate the one-third octave band spectrum for each acoustic roughness record (amplitude of the acoustic roughness expressed as a function of the wavelength λ), and, finally, estimate the same spectrum in dB. The technique of spectral analysis adopted for road profiles to treat the rail profiles was used [28].

An example of Wavelength-RMS disp graph is shown in Fig. 8. Central frequencies in the calculus are chosen, the same as the International Standard ISO 8608:1995 [29] provides, and to create, in a numerical way, a one-third octave band spectrum, the Technical Specification ISO/TS 13473-4 [30] about Spectral analysis of surface profiles was followed. To select the alternative method (Method B), the one-third octave band values shall be obtained by applying digital one-third octave band filters directly to the roughness data.

The obtained spectrum $\lambda - \tilde{r}(\lambda)$ thus can be compared with standard limits according to the needs: limits that are not univocally established if not for rail used during

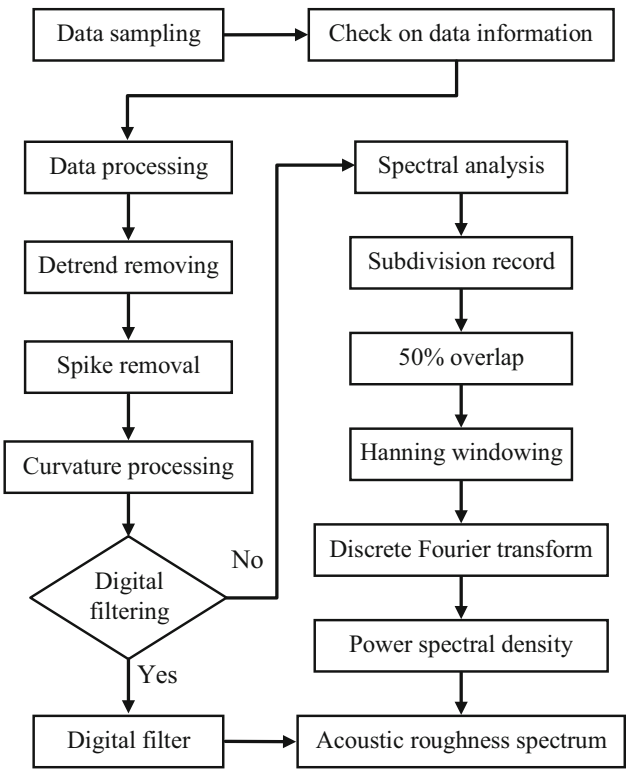

Fig. 7 Algorithm of the method (UNI EN 15610:2009) [27]

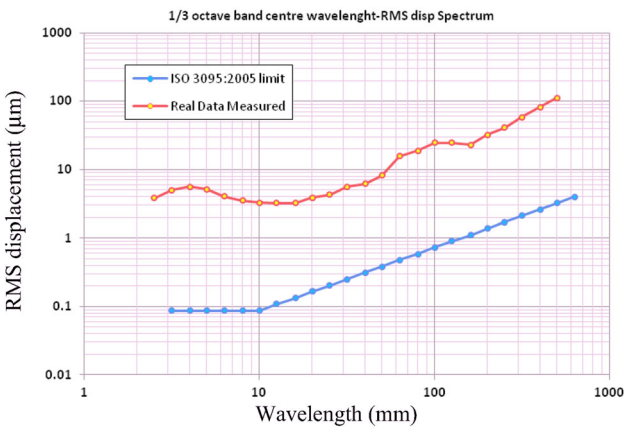

Fig. 8 One-third octave band spectrum calculated through the algorithm proposed by ISO 8608 [29], on a recorded measure in a depot of rolling stock

vehicle-type testing (Technical Specifications for Interoperability, Decision 2006/66/EC, [31]) or for measurement of noise emitted by rail-bound vehicles (ISO 3095:2005, [32]), and particularly for railway field [12].

Figure 9 shows both acoustic roughness spectra of a tramway rail and standard limits for railway rail.

To calculate the acoustic roughness spectrum the following steps are necessary:

- Detrend removing process: to remove the best straight-line fit from distance vector.
- Spike removal process: to remove narrow upward spikes that are regarded as being linked with the presence of small particles of foreign matter on the rail surface; identify the spikes by the criteria $d^2r/dx^2 < -10^7$ μm/m^2 and a change of sign for dr/dx, calculate the first and the second derivative of $r(x)$, the roughness acoustic vector, identify the edges of each spike as being the extreme points (x_1 and x_2) on either side of the maxima or minima, for which $abs(dr/dx)$ becomes less than 5×10^3 μm/m; calculate the width w of the spike with the formula $w = abs(x_2 - x_1)$, and where $h > w^2/a$ (h = height of the spike, a = 3 m) spike shall be removed by linear interpolation between x_1 and x_2.
- Curvature process: to account for the effect of the small radius of the probe tip compared to that of the wheel, taken as the $r'(x_i)$ obtained from the sum between the maximum values intercepted in the difference $r(x) - C_i(x)$ (in particular the roughness function $r(x)$ and the curve $C_i(x)$, r = 0,375 m, centered at x_i above $r(x)$ function), and the $r(x_i)$, the roughness value in that specific i (Fig. 10).
- Windowing: to avoid discontinuity at the edges of each discrete signal due to the DFT is based on the hypothesis that the input discrete signal repeats itself with a period equal to the signal length. The single signals may be linked only if at the edges of each discrete signal, there are the same values equal to zero. The windowing reduces the signal to zero at the edges limiting the attenuation of the signal out of the edges. In general, the equation for determining the windowed profile $Z_{i,\text{win}}$ starting from original profile Z_i is given:

$$Z_{i,\text{win}} = \frac{w_i Z_i}{\sqrt{\frac{1}{N}\sum_{i=0}^{N-1} w_i^2}} \quad \text{for } i = 0, 1, \ldots, N-1, \tag{1}$$

where w_i is a set of coefficients that changes the original profile minimizing the unexpected effect known as "leakage".

- Discrete Fourier Transform (DFT): for the rail profile, according to the classic utilization for a time-domain signal, DFT involves a transformation from the distance domain (in m) to the frequency domain, in particular spatial frequency domain (in cycle/m or $1/\lambda$ where λ is the wavelength). The result of the DFT is a constant bandwidth narrow band spectrum Δf with complex values, calculated by:

$$Z_k = \frac{1}{N}\sum_{i=0}^{N-1} Z_{i,\text{win}} e^{-j\left(\frac{2\pi k}{N}\right)i}, \tag{2}$$

where j imaginary unit, $j^2 = -1$ used for transform the N real numbers $Z_{i,\text{win}}$, i = 0,1,…,N-1, in N complex numbers Z_k, k = 0,1,…,N–1. The bandwidth Δf depends on the discrete profile length $L = (N-1)\Delta x$ and is equal to:

$$\Delta_f = \frac{1}{L}. \tag{3}$$

The spatial frequency scale of Z_k starts at 0 with steps equal to Δf until $f_{max} = (N/2 - 1)\Delta f$. The others Z_k complex values shall be not used because this function is symmetrical.

- Power spectral density (PSD): PSD function shows the frequency distribution of the power associated with the signal per unit frequency. PSD is obtained by dividing

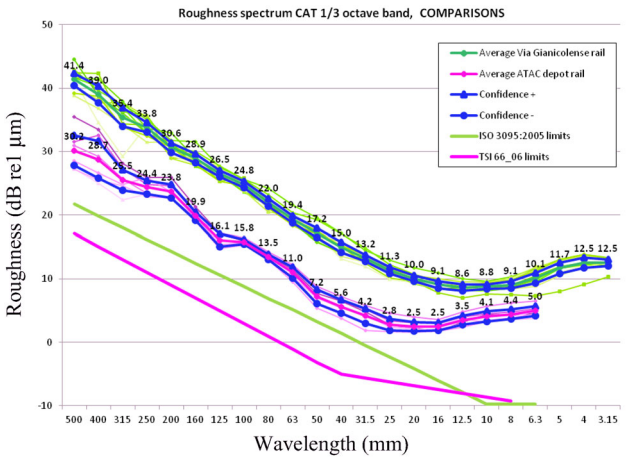

Fig. 9 Example of roughness spectra (whose values are given in dB ref. 1 μm) of standard limit curves and of measures carried out with the corrugation analysis trolley

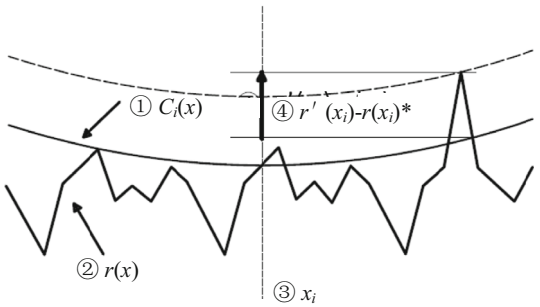

* $r'(x_i)$=max[$r(x)$-$C_i(x)$]+$r(x_i)$

Fig. 10 Criterion applied to position x_i

the squared amplitude of each narrow band by the spectral bandwidth Δf according to equation:

$$Z_k^{\mathrm{PSD}} = \frac{2|Z_k|^2}{\Delta f} \text{ for } k = 0, 1, \ldots, \left(\frac{N}{2} - 1\right), \tag{4}$$

expressed in $\mathrm{m}^2/\mathrm{m}^{-1} = \mathrm{m}^3$.

- Roughness spectrum: a constant bandwidth spectrum to summarize the frequency content of the signal (that is specifically the longitudinal profile) is created. A one-third octave band spectrum shall be synthesized on the basis of the narrow band spectrum. Each one-third octave band value shall be calculated as the energy sum of the narrow band values from the DFT. The same signal examined in third-octave bands can evidence the presence of maxima or minima of the acoustic roughness levels that in octave bands would not be visible, providing more detailed information. The bands are sets of frequencies characterized by constant percentage bandwidth: calling the center frequency f_c and f_l (low) and f_h (high) frequencies below and above, for an octave band is delimitated with respect to the following equation:

$$\frac{f_h - f_l}{f_c} = \frac{1}{2^{1/2}}. \tag{5}$$

The exponent 1/6 is used to define the one-third octave band.

To filter the signal of profiles, a Butterworth filter can be used.

The Butterworth filter is a type of signal-processing filter designed to have more flat frequency response in the pass band.

The function of power spectral density (in frequency domain) is

$$A^2(\omega) = k^2/1 + (\omega/\Omega)^{2n}, \tag{6}$$

where ω is related to frequency through the relation $\omega = 2\pi f$ and the max value of $A(\omega)$ is in $\omega = 0$, where it is just equal to the constant k. The integer n is called "order" of the filter, and Ω is the cutoff frequency (approximately the -3 dB frequency).

To design a numerical Butterworth filter a simple code written in MATLAB® has been used.

The order of the filter and the cutoff frequency W_n should be defined in advance in the code (here, the filter is designed to be a $2n$-order filter).

Figure 11 shows the magnitude and phase responses of the 6th order Butterworth filter.

The acoustic roughness level is given by the following expression:

$$L_r = 10\log\left(r_{\mathrm{RMS}}^2/r_0^2\right), \tag{7}$$

where

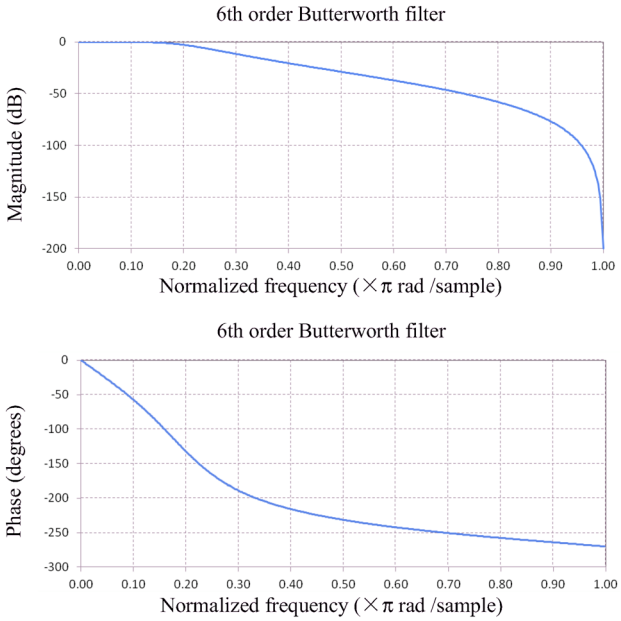

Fig. 11 Magnitude and phase responses of the 6th order bandpass filter used to analyze the displacement signal with cutoff frequency of 200 cycles/m (corresponding to $\lambda_{\min} = 5$ mm)

- L_r is the acoustic roughness level in dB,
- r_{RMS} is the root mean square of rail roughness in μm,
- r_0 is the reference of rail roughness ($r_0 = 1$ μm).

Using this decibel scale, a roughness value of 1×10^{-6} m = 0 dB, 3.2×10^{-6} m = 10 dB, 10×10^{-6} m = 20 dB, etc. [34].

6 Evaluating profilometric data by means of percentage exceedance

Another evaluation criterion used for the analysis of the profiles is the method of "*percentage exceedance*". For each reference interval λ, the curves of cumulative frequency are constructed compared with amplitude values expressed in microns RMS. For example, in Fig. 12, the red curve shows the corrugation range 30–100 mm. For a displacement of 20 μm (RMS) corresponds an exceedance more than 45 % on the rail and for a displacement of 40 μm (RMS) corresponds an exceedance by around 15 %. Such information may be used as a reference for management of rail grinding.

This procedure is given in Annex C of the standard on the acceptance of the quality of grinding work (UNI EN 13231-3:2012, [35]).

7 Assessment of profilometric data by means of expeditious methods

Some administrations of public transport, for each meter of profile recorded, decide the need for grinding the rail if the

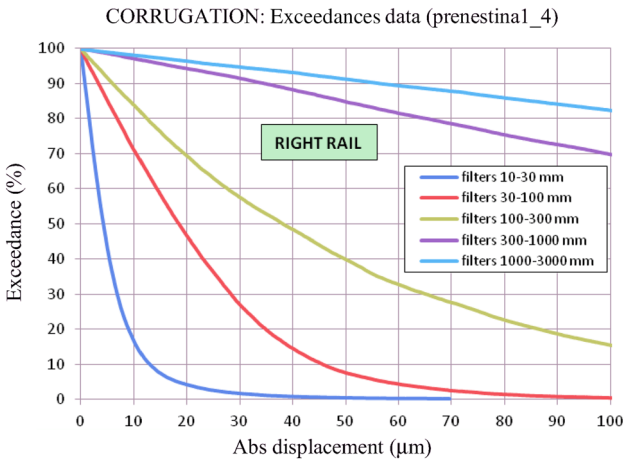

Fig. 12 Graph of the percentage exceedance on a tramway section in Rome

defect height exceeds the limits of 0.3–0.4 dmm with 8–10 cm of wavelength.

A tram rail section, by about 60 m, was measured by means of CAT. The profile recording, filtered in the range of wavelength λ=30–100 mm, is shown in Fig. 13a. In Fig. 13b, a 1 m long sub-section is produced, showing the trend that remains under the displacements of ±300 µm.

8 Case study

As part of a Research Project some segments of tram network in Rome were detected, which are characterized by different levels of rail corrugation. The instrumentation used in measurement is the Corrugation Analysis Trolley and the profile measurements were conducted with three evaluation methods presented in the above sections.

Figures 14, 15, and 16 show the main results about the profilometric data recorded on a corrugated rail in Via Gianicolense.

Figure 14 shows a comparison between the acoustic roughness spectrum and the TSI 2006/66/EC [31] limit curve in magenta (or the ISO 3095 [32] limits in green, the TSI 2002/735/EC [33] limits dashed line). Figure 15 shows the percentage exceedance graph, with the 50 % line highlighted, and Fig. 16 shows profilometric measure of 1 m in the wavelength range of 30–100 mm.

The examined rail exceeds limits if compared with limit curves supplied for railway field (due to the higher speed of the trains).

According to the second way to evaluate the condition of the rail, in the Fig. 15, it can be seen that 50 % of the length of the track shows an amplitude of irregularity with magnitudes less than 10 µm. The same percentage does not

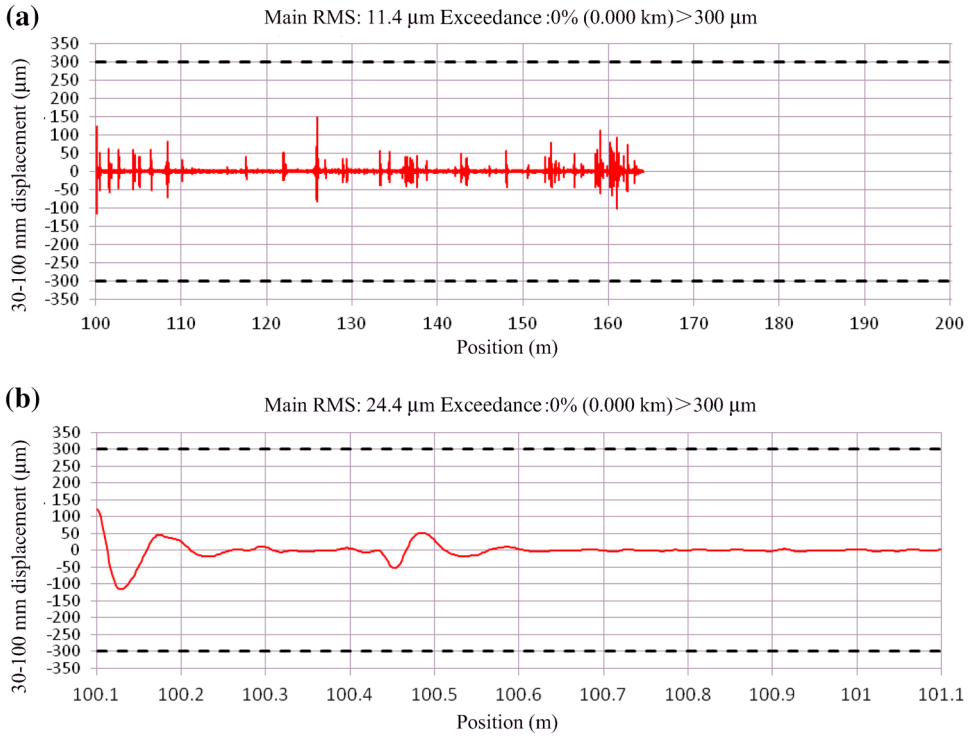

Fig. 13 Profile recording filtered in the range of wavelength λ = 30–100 mm (**a**) and a section (1-m long) of the profile (**b**) (the *dashed lines* indicate the thresholds of ±300 µm)

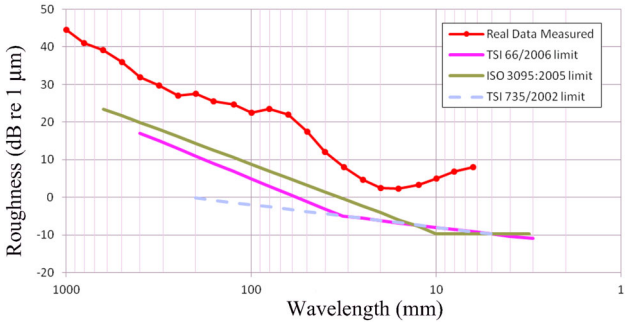

Fig. 14 Acoustic roughness spectrum compared with standard limits curves

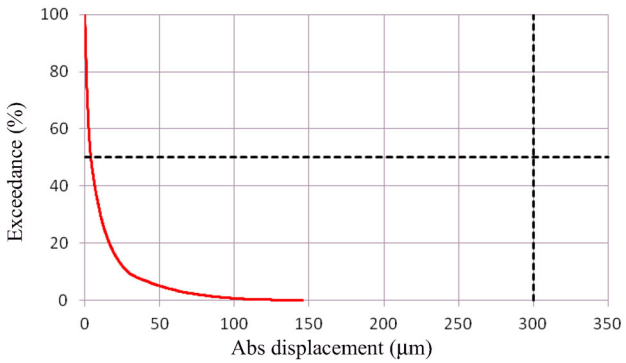

Fig. 15 Percentage exceedance graph

correspond any point of the exceedance curve: for example there is no correspondence at an amplitude of the irregularity with magnitude of 300 µm.

At last, using the third way to evaluate the profilometric data, the assessment of the measured section reveals that, for the range $\lambda = 30$–100 mm, the displacement does not exceed 300 µm in the overall recording.

9 Discussion and conclusion

During the service life, each railhead is inevitably subjected to damaging. Within the several manifestations in which the damages can occur on the running surface, the most discussed in this paper are the periodic irregularities.

The particular attention to these types of defects is due to the acknowledged link existing between the corrugation of the rail surface and the generation of noise and vibrations (the corrugation interests also the surface of the wheels and naturally leads to an exacerbation of the phenomenon, but this is not discussed in this paper).

In the contact area, wheel and rail exchange interaction forces: the presence of irregularities on the running surfaces arises from dynamic loads, that, besides getting worse the damaged surface initiates vibrations of vehicle and track components (the formation of periodic surface defects is also accelerated by the speed-up of trains [36]).

Even an interaction between not-worn wheels and rails generates dynamic forces, due to the track configuration itself (e.g., the sleepers are supporting the rail with a specific spacing; they do not represent a uniform base for the vehicle riding).

Rail corrugation, a particular kind of periodic wear discussed in this paper, is one of the most serious problems in railway engineering. Its formation and development cause high level of vibrations between railway vehicle and track, noise and reduction of the useful life of the structural parts. Sometimes serious corrugation of rail leads to derailments [37].

The purpose of monitoring and diagnostics is to control the structural integrity, ensure no alteration of structural components, keep the performances of the railway/tramway, and provide a useful pretext for the policy decisions of the interventions. Monitoring of rail irregularities represents, indeed, an investment to manage the evolution of the track damage; for example, it can be a chosen optimal to minimize the use of interventions in urgent cases, reducing the inefficiencies of the transport system only to planned interventions.

Dedicated equipment, and more in detail the manual corrugation measurement device CAT (specifically developed for the measurement of corrugation), have been described in this paper, together with three different methods to assess the profilometric data recorded.

The three evaluation methods for treating longitudinal irregularity recordings, all of them examined for the same section of tram rail, show contrasting results: the most rigorous method, which leads to gain the *Acoustic Roughness Spectrum* to compare with some reference levels provided by standards, is not very useful since the tram rails have always significantly accentuated longitudinal irregularities. Acoustic roughness spectrum calculated for a tram rail is always over the standard limit spectrum. Therefore, new limits should be established ad hoc for the tram rails, which are subject to operating conditions that are much more critical than the railway rails ones.

In this paper, the method for calculating the acoustic roughness spectrum has been developed starting from the profiles of the rails measured with the CAT. This methodology is entirely in line with the Standard UNI EN 15610:2009 [27] and it applies some algorithm and procedure used also to treat the road profiles.

The second method, which involves the determination of the curve *Percentage Exceedance*, seems to be very interesting: in an easy way can be read the whole range of irregularities found on the rail surface, highlighting the one with higher rate of presence. Though, unfortunately, the

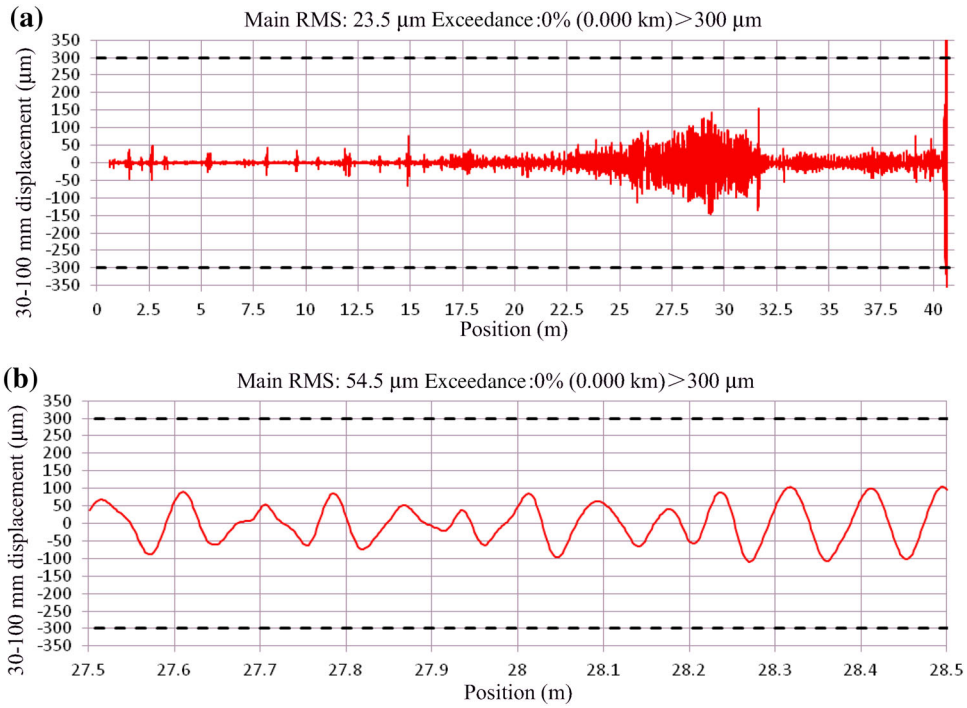

Fig. 16 Profile recorded in via Gianicolense (**a**) and its selection of one-meter long (*bottom*) (**b**) in the wavelength range of $\lambda = 30$–100 mm (thresholds ±300 µm)

height thus obtained is not associated with its own wavelength (but the wavelength range of interest, which includes various profile components).

The third method, which assumes to provide the maximum amplitude of irregularities associated with a single wavelength, is the easiest method, and it is currently most used by managers of tram networks, to assess the status of the rails. This method, certainly expeditious, focuses only on one type of defect of the rail and can lead to erroneous evaluations and interpretations.

Acknowledgments The Corrugation Analysis Trolley (CAT) mentioned in this paper, is owned by ATAC S.p.a. (ATAC is the Italian acronym that stands for *Agenzia per la Mobilità del Comune di Roma*, which is the agency that manages the Public transport in Rome) and it has been lent for temporary use to DICEA, to perform some collaborative research project.

References

1. Kalker JJ (1980) Review of wheel-rail rolling contact theories, American Society of Mechanical Engineers. Appl Mech Div 40:77–91
2. Johnson KL (1987) Contact mechanics. Cambridge University Press, Cambridge
3. Lewis R, Olofsson U (2009) Wheel-rail interface handbook. CRC Press, Oxford
4. Oostermeijer KH (2006) Short pitch rail corrugation-cause and contributing factors. In: 7th World Congress on Railway Research (WCRR), Montréal
5. Popovici RI (2010) Friction in wheel-rail contacts. Dissertation, University of Twente, Enschede
6. Ringsberg JW (2001) Life prediction of rolling contact fatigue crack initiation. Int J Fatigue 23(7):575–586
7. Grassie SL (2012) Squats and squat-type defects in rails: the understanding to date. Proc Inst Mech Eng Part F 226(3):235–242
8. Steenbergen MJMM (2008) Quantification of dynamic wheel–rail contact forces at short rail irregularities and application to measured rail welds. J Sound Vib 312(4–5):606–629
9. Wu TX, Thompson DJ (2005) An investigation into rail corrugation due to micro-slip under multiple wheel/rail interactions. Wear 258(7–8):1115–1125
10. Iwnicki S (2006) Handbook of railway vehicle dynamics. CRC Press, Boca Raton
11. Thompson DJ (1996) On the relationship between wheel and rail surface roughness and rolling noise. J Sound Vib 193(1): 149–160
12. Grassie SL (2012) Rail irregularities, corrugation and acoustic roughness: characteristics, significance and effects of reprofiling. Proc Inst Mech Eng Part F 226(5):542–557
13. Bonin G, Cantisani G, Carbonari M, Loprencipe G, Pancotto A (2007) Railway traffic vibrations: generation and propagation-theoretical aspects. In: 4th International SIIV Congress, Palermo
14. Zoccali P, Cantisani G, Loprencipe G (2015) Ground-vibrations induced by trains: filled trenches mitigation capacity and length influence. Constr Build Mater 74:1–8. doi:10.1016/j.conbuildmat.2014.09.083
15. Curcuruto S, Atzori D, Betti R, Marsico G, Mazzocchi E, Monaco E, Amoroso F, Limone V, Loprencipe G, De Felice F (2012) Propagation of vibration induced on track:

Implementation of previsional models for low and high speed trains and comparison with experimental measurements. In: 19th International Congress on Sound and Vibration 2012, ICSV 2012, 4:3033–3040
16. Di Mascio P, Loprencipe G, Maggioni F (2014) Visco-elastic modeling for railway track structure layers [Modellazione del comportamento visco-elastico degli strati della sede ferroviaria]. Ingegneria Ferroviaria 69(3):207–222
17. Grassie SL (2005) Rail corrugation: advances in measurement, understanding and treatment. Wear 258(7):1224–1234
18. Nielsen JCO, Johansson A (2000) Out-of-round railway wheels-a literature survey. Proc Inst Mech Eng Part F 214(2):79–91
19. Grassie SL (2009) Rail corrugation: characteristics, causes, and treatments. Proc Inst Mech Eng Part F 223(6):581–596
20. Lichtberger B (2005) Track compendium- formation, permanent way, maintenance, economics. Eurail Press, Hamburg
21. Daniel WJT, Horwood RJ, Meehan PA, Wheatley N (2008) Analysis of rail corrugation in cornering. Wear 265(9–10):1183–1192
22. Brickle BJ, Elkins JA, Grassie SL, Handal SJ (1998) Rail corrugation mitigation in transit, Research Results Digest, Transit Cooperative Research Program, National Research Council
23. Grassie SL, Edwards JW (2008) Development of corrugation as a result of varying normal load. Wear 265(9–10):1150–1155
24. Nielsen JCO (2008) High-frequency vertical wheel-rail contact forces-validation of a prediction model by field testing. Wear 265(9–10):1465–1471
25. Jones CJ, Létourneaux F, Fodiman P (2008) Testing a new rail roughness measurement standard. J Acoust Soc Am 123(5):3266
26. Bongini E, Grassie SL, Saxon MJ (2012) "Noise mapping" of a railway network: validation and use of a system based on measurement of axlebox vibration. In: Maeda T, Gautier PE, Hanson CE, Hemsworth B, Nelson JT, Schulte-Werning B et al (eds) Noise and vibration mitigation for rail transportation systems. Springer, Japan, pp 505–513
27. Ente Italiano di Normazione. UNI EN 15610:2009 Railway applications—Noise emission—Rail roughness measurement related to rolling noise generation
28. Loprencipe G, Cantisani G (2013) Unified analysis of road pavement profiles for evaluation of surface characteristics. Mod Appl Sci 7(8):1–14. doi:10.5539/mas.v7n8p1
29. International Organization for Standardization, Mechanical vibration—Road surface profiles—Reporting of measured data, ISO 8608:1995 (E), 09 Jan 1995
30. International Organization for Standardization—Technical specification, characterization of pavement texture by use of surface profiles—part 4: Spectral analysis of surface profiles, ISO/TS 13473-4:2008 (E), 05 Jan 2008
31. European Commission, Technical specification for interoperability relating to the subsystem 'rolling stock—noise' of the trans-European conventional rail system, TSI 2006/66/EC, 23 Dec 2005
32. European Committee for Standardization, Railway applications—Acoustics—Measurement of noise emitted by rail bound vehicles, EN ISO 3095:2005 (E), 31 Jan 2006
33. European Commission, Technical specification for interoperability relating to the rolling stock subsystem of the trans-European high-speed rail system referred to in Article 6(1) of Directive 96/48/EC, TSI 2002/735/EC, 30 May 2002
34. Hardy AEJ, Jones RRK (2004) Rail and wheel roughness-implications for noise mapping based on the calculation of railway noise procedure. AEA Technol Rail 1:46–52
35. European Committee for Standardization, Railway applications—Track—Acceptance of works—part 3: Acceptance of reprofiling rails in track, EN 13231-3:2012 (E), 29 Feb 2012 (accepted in the national standards bodies of Italy from the organization "Ente Nazionale Italiano di Unificazione" as UNI EN 13231-3:2012)
36. Sato Y, Matsumoto A, Knothe K (2002) Review on rail corrugation studies. Wear 253(1–2):130–139
37. Jin X, Wen Z, Wang K, Zhang W (2004) Effect of high-frequency vertical vibration of track on formation and evolution of corrugations. Tsinghua Sci Technol 9(3):274–280